AGU ADVANCING EARTH AND SPACE SCIENCES

Geophysical Research Letters

RESEARCH LETTER
10.1029/2026GL121625

Windblown Diatoms for Reconstructing Westerly Wind Variability in the South Atlantic Sector of the Southern Ocean

Dieter R. Tetzner[1], **Elizabeth R. Thomas**[1], **Claire S. Allen**[1], **Delia Segato**[2,3], **and Shaun Miller**[1]

[1]British Antarctic Survey, Ice Dynamics and Paleoclimate, Cambridge, UK, [2]European Commission Joint Research Centre, Ispra, Italy, [3]Department of Environmental Sciences, Informatics and Statistics, Ca' Foscari University of Venice, Venice-Mestre, Italy

Key Points:

- Windblown diatoms found in the firn of Bouvet Island provide a record of pristine and locally sourced marine taxa from the Southern Ocean
- Correlation analyses reveal that Bouvet's interannual diatom abundance variability is primarily driven by westerly wind strength changes
- The diatom record from Bouvet Island serves as a proxy for reconstructing past westerly wind belt variability in the South Atlantic

Supporting Information:

Supporting Information may be found in the online version of this article.

Correspondence to:

D. R. Tetzner,
dietet95@bas.ac.uk

Citation:

Tetzner, D. R., Thomas, E. R., Allen, C. S., Segato, D., & Miller, S. (2026). Windblown diatoms for reconstructing westerly wind variability in the South Atlantic sector of the southern ocean. *Geophysical Research Letters*, *53*, e2026GL121625. https://doi.org/10.1029/2026GL121625

Received 7 JAN 2026
Accepted 27 MAY 2026

Author Contributions:

Conceptualization: Dieter R. Tetzner
Data curation: Dieter R. Tetzner
Formal analysis: Dieter R. Tetzner, Elizabeth R. Thomas, Claire S. Allen, Delia Segato
Funding acquisition: Elizabeth R. Thomas
Investigation: Dieter R. Tetzner, Claire S. Allen, Delia Segato
Methodology: Dieter R. Tetzner, Claire S. Allen, Delia Segato
Project administration: Elizabeth R. Thomas
Resources: Shaun Miller
Validation: Dieter R. Tetzner
Visualization: Dieter R. Tetzner

Abstract Southern Hemisphere westerly winds are important drivers of Antarctic and sub-Antarctic environmental change. Short observational wind records prevent us from fully understanding the scope of their variability. Proxy records provide valuable tools to extend environmental records. Here we present a novel wind study based on the use of windblown diatoms preserved in layers from the first firn core drilled in the sub-Antarctic Bouvet Island. The firn core diatom record is comprised of high-concentrations of pristine and locally sourced Southern Ocean marine taxa. This record is the first to characterize the diatom diversity and abundance actively entrained by winds in the sub-Antarctic region. Correlation analyses reveal interannual diatom abundance variability is primarily driven by wind strength changes in the core of the westerly wind belt. These results validate using the Bouvet Island diatom record as a proxy for reconstructing past atmospheric circulation variability over the Atlantic sector of the westerly wind belt.

Plain Language Summary Southern Hemisphere westerly winds are important drivers of Antarctic and sub-Antarctic environmental changes. However, we do not have enough information about how these winds change over time. Proxy records help us extend our knowledge of environmental changes. In this study, we examine windblown phytoplankton preserved in ice layers from the sub-Antarctic Bouvet Island. Our analysis indicates that changes in wind strength within the westerly wind belt mostly drive the yearly variations in phytoplankton abundance. These results support the use of the Bouvet Island phytoplankton record as a proxy to understand past changes in atmospheric circulation over the Atlantic sector of the westerly wind belt.

1. Introduction

The Southern Hemisphere Westerly Winds (SHWWs) play an important role in modulating the Antarctic ice sheet volume (Medley & Thomas, 2019; Pritchard et al., 2009) and mediating the ocean-atmosphere carbon dioxide exchange (Gruber et al., 2019; Le Quéré et al., 2007). SHWWs have been strengthening and shifting poleward in recent decades (Jones et al., 2016) and have been proposed among the main drivers of observed environmental changes in Antarctica and the sub-Antarctic region (Perren et al., 2020). These SHWW trends are predicted to continue (Deng et al., 2022) and are expected to impact the efficiency of the Southern Ocean (SO) carbon sink (Keppler & Landschützer, 2019). Despite their relevance, the lack of long-term SHWW records hinders our ability to assess the wider context of the recent changes and predict future system responses.

Paleoclimate archives yield a wealth of past environmental information inferred from proxy records. Several archives have been explored to reconstruct SHWWs (e.g., Lake sediments, peat-bogs, ice cores, etc.) (Koffman et al., 2023; Saunders et al., 2018; Tamhane et al., 2023). Nevertheless, most of these records rely on indirect environmental proxies to infer SHWWs changes, using proxies that are often affected by conditions at the source region (e.g., Flores-Aqueveque et al., 2024) or only provide information at decadal to centennial timescales. There is an acute need for more direct SHWW proxies and annual resolution records.

Marine diatoms (unicellular algae) preserved in Antarctic Peninsula ice core layers have been established as a reliable proxy for reconstructing past changes in wind strength in the Pacific sector of the SHWW belt (Allen et al., 2020; Tetzner, Allen, & Thomas, 2022; Tetzner, Allen, et al., 2025). Strong winds entrain diatoms from the sea surface, transport them over long distances and deposit them along their pathway (Budgeon et al., 2012;

Writing – original draft: Dieter R. Tetzner
Writing – review & editing: Dieter R. Tetzner, Elizabeth R. Thomas, Claire S. Allen, Delia Segato

Harper & McKay, 2010). Despite the potential of this proxy, it has not yet been tested in the Sub-Antarctic, the prime source region of the windblown diatoms.

Bouvet Island (Bouvetøya, a Norwegian dependency) is a remote, ice-covered, Sub-Antarctic island located in the Atlantic sector of the SO (Figure 1a). Currently, this 49 km^2 volcanic island is one of the few islands that sit within the core of the SHWW belt (Figure 1b; Thomas et al., 2021) and an ideal site to track past changes in SHWWs. In 2017, the Antarctic Circumpolar Expedition recovered the first-ever firn core from the island (Thomas et al., 2021), providing an unrivalled opportunity to explore the diatom record from ice deposited in the core of the SHWWs.

Here we present the diatom record preserved in the Bouvet Island firn core, including (a) annual and sub-annual diatom abundance to determine the temporal variability in diatom content, and (b) diatom ecological affinity and air mass back trajectory analyses, to identify primary diatom source regions. We use this information to evaluate the diatom record's potential to reconstruct past SHWW changes in the region and the potential influence of sea ice and primary productivity in driving diatom variability in the ice.

2. Methods

2.1. Firn Core Drilling Site and Chronology

The Bouvet Island firn core (BOU, 14.2 m) was drilled using a Kovacs Coring System during March 2017. The BOU drilling site (54°25′19″S, 3°23′27″E) was located on the eastern side of the island at 350 m above sea level (m a.s.l.) (Figure 1a; Thomas et al., 2021). A BOU chronology was established based on annual cycles of stable water isotopes and major ions (King et al., 2019). The firn core base was dated back to austral winter 2000 CE (King et al., 2019) and includes thin melt layers (mean 0.3 cm; Thomas et al., 2021).

2.2. Diatom Sample Preparation and Analyses

The BOU was cut using a steel-bladed bandsaw in the cold laboratories at the British Antarctic Survey, UK. An ice strip (1.7 cm × 3.4 cm) was subsampled for diatom analysis at an annual resolution based on the BOU ice chronology (King et al., 2019). A missing section of firn in the strip from the first core bag prevented accurately resolving the position of the 2016 winter horizon. Therefore, for consistency, the diatom record covers the interval between austral winters 2000–2015 CE. Ice from the five annual layers (austral winter-to-winter; closest to mean accumulation), was split to obtain sub-annual samples: 2003–2004, 2005–2006, 2011–2012, 2013–2014, and 2014–2015 CE, to assess intra-annual variations in the diatom record. The sub-annual record presented in this work considered each sample as seasonal, assuming constant snow deposition in the BOU site throughout the year. Each set of four sub-annual samples were totaled to provide annual values for these targeted years.

After cutting, all diatom samples were individually melted and then extracted by filtration. The meltwater samples were filtered through a polycarbonate membrane filter (pore diameter 1.0 μm) and subsequently scanned at x800 magnification in a scanning electron microscope (SEM) at the University of Cambridge, following the method and recommendations presented in Tetzner et al. (2021). Observations regarding diatom preservation were based on characteristic frustule dissolution and degradation presented by Warnock and Scherer (2015). Diatom valves and fragments with a long axis of less than 5 μm were excluded from the diatom counting and identification due to image resolution limitations.

Diatom counts per sample (n) included all diatom valves, partially covered diatom valves, and fragments identified in each sample, regardless of their potential source. This parameter was then transformed to diatom abundance ($n\ t^{-1}$), where t represents the temporal resolution of each sample (e.g., year, season). To compare diatom abundance with other ice core sites, a diatom concentration ($n\ L^{-1}$) parameter was calculated by normalizing the diatom counts per sample (n) with the meltwater volume (L) filtered per sample. Diatom abundance was correlated with L and snow accumulation estimated from BOU (King et al., 2019) to measure interdependence between variables. All correlations were calculated using Pearson's linear correlation (R). When calculating correlations, the diatom abundance parameter was linearized by applying the natural log to the data set. Linearized diatom abundance values above the median plus two standard deviations were considered outliers and removed while conducting correlation calculations. Additionally, all data sets were processed using linear detrending before calculating correlations.

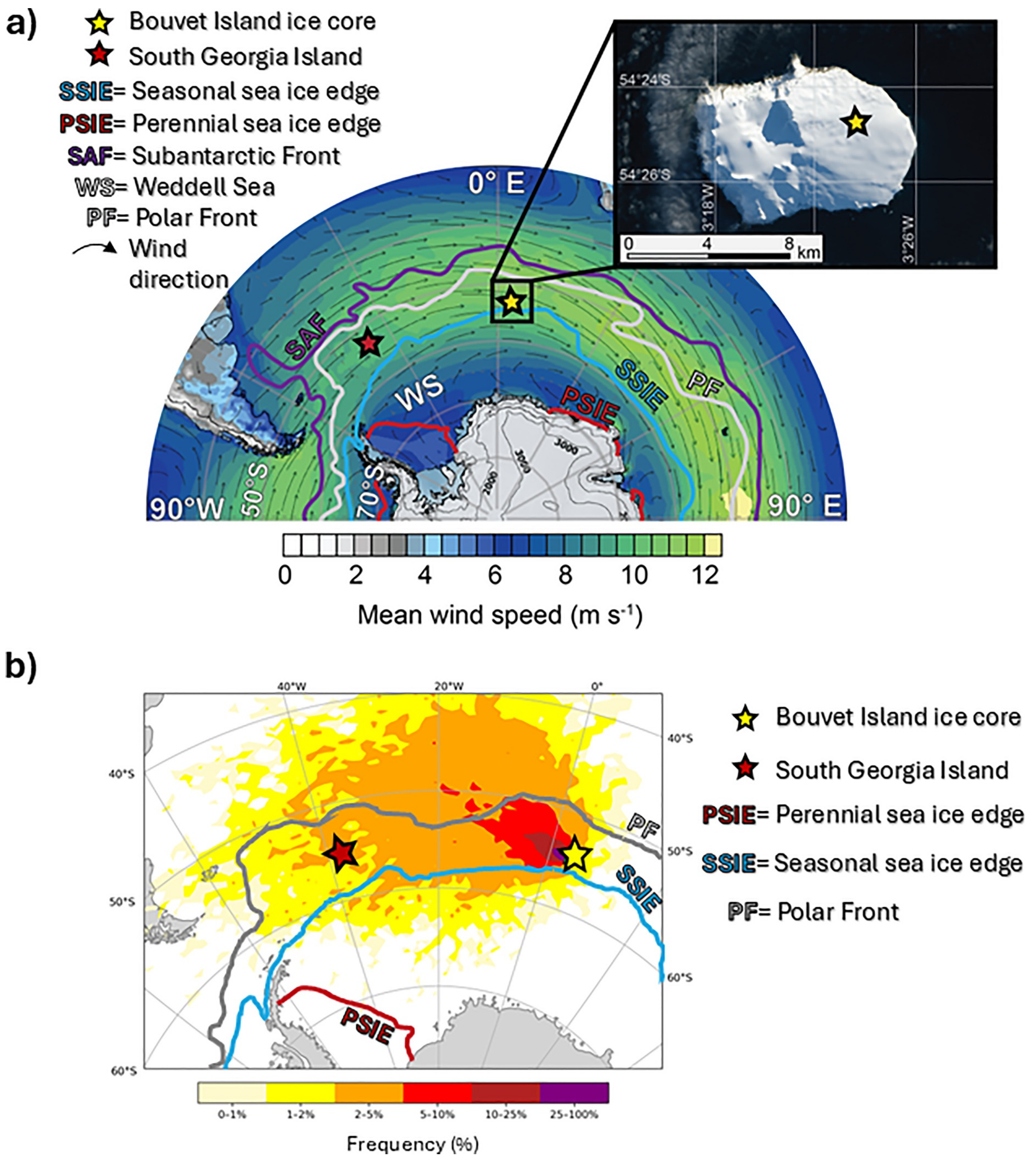

Figure 1. Maps of Antarctica and the SO. (a) ERA5 mean wind speed (2000–2015 CE) over the SO. Insert map shows a satellite image (Landsat 8) of Bouvet Island. (b) Spatial density of all 5-day trajectories interacting with the surface ocean and reaching Bouvet Island (2005–2015 CE).

Diatom identification and ecological associations were based on Armand et al. (2005), Halse et al. (1996), Cefarelli et al. (2010), Zielinski and Gersonde (1997) and references therein. Diatoms were identified to species level where possible. Diatoms that were not suitable for species level identification, were combined in generic/morphological groups. All remaining specimens (e.g., no diagnostic features, poorly ornamented, indistinct, or obscured) (Figure S1 in Supporting Information S1) were omitted from ecological associations and assemblage composition but were included in the total diatom counts (n). The diatom assemblage composition was determined from the identified species and groups with abundances higher than 2.0% of the total diatom record. Ecological associations were determined for the most abundant species/groups.

Ice core diatom records from Antarctic Peninsula low-elevation coastal sites are highly influenced by the presence of sea ice diatoms (Tetzner, Thomas, et al., 2022). A sea ice diatom index (SIDI) was calculated to study annual and sub-annual relations between the total diatom abundance (concentration), the sea ice diatom abundance (concentration), and the non-sea ice diatom abundance (concentration). The SIDI was calculated for each sample as the sum of the diatom abundance (concentration) of the two characteristic sea ice diatoms in the SO: *Fragilariopsis cylindrus* and *F. curta* (Cefarelli et al., 2010; Lizotte, 2001). *Fragilariopsis cylindrus* may also include F. *nana* specimens (Cefarelli et al., 2010). The non-sea ice diatom abundance (concentration) index (n-SIDI) was calculated as the residual after removing SIDI from the total diatom abundance (concentration) of each sample. Within the n-SIDI parameter, diatoms identified as *Pinnularia* cf. *borealis* may also include minor contributions of *Achnanthes* spp., and diatoms identified as *Thalassiothrix* group, formed by *Thalassiothrix* spp., *Thalassionema* spp., and *Trichotoxon reinholdii*, may also include minor contributions of *Synedra* spp.

2.3. Climate Reanalyses, Sea Ice Edge Position and Chlorophyll Concentration Data

Monthly reanalysis fields from ERA5 (Hersbach & Dee, 2016), were used to perform spatial correlations between the BOU annual diatom abundance records (total, SIDI and n-SIDI) and five environmental variables: 10-m height winds (speed, zonal and meridional components (m/s)), sea level pressure (hPa) and sea ice cover (% of grid box). ERA5 data sets provide hourly data available at 0.25° resolution (∼31 km) since 1979 CE and have been proven reliable at capturing wind and climate variability over coastal Antarctic regions and other sub-Antarctic islands (Tetzner et al., 2019; Thomas et al., 2024). ERA5 annual mean wind speed over a 5° × 5° area (Figure S2 in Supporting Information S1) centered on Bouvet was calculated to correlate with the annual total diatom abundance record.

Sea Ice edge daily data set from the Copernicus Climate Change Service (C3S) (Araboe et al., 2023) was used to obtain the annual northernmost position of the sea ice edge at 12.5 km resolution (2000–2015 CE). The sea ice edge is defined as the northern limit of the 30% sea ice concentration. A 10° × 10° area (∼1,400,000 km^2) centered on Bouvet was selected to study the maximum sea ice extent around the island (Figure S2 in Supporting Information S1). The maximum sea ice extent near Bouvet Island occurs between September and October. The September-October northernmost sea ice edge data set was used to calculate a local correlation with the diatom data sets. The October sea ice cover was used to calculate spatial correlations as it represents the onset of the sea ice breakup, which increases the productivity of sea ice diatoms (Riaux-Gobin et al., 2011).

Chlorophyll concentration data from NASA's Aqua-MODIS satellite was used to obtain monthly and annual chlorophyll concentration at 9 km resolution (2002–2015 CE). Chlorophyll concentration is directly related with primary productivity (Moore & Abbott, 2000) and included here to explore its relationship with the Bouvet Island diatom record. Mean chlorophyll concentrations were calculated over two latitudinal bands around Bouvet (Figure S2 in Supporting Information S1); (a) an extended region including Bouvet and South Georgia Island (50–60°S, 45°W–10°E), and (b) a reduced region only surrounding Bouvet Island (50–60°S, 10°W–10°E). These areas were selected to incorporate data sets with and without the influence of the South Georgia bloom (Soppa et al., 2016). Correlations were performed using annual mean and annual maximum (highest monthly mean for the whole region) chlorophyll concentration values.

2.4. Backward Trajectory Analyses

Backward trajectory analysis is used to trace the pathways followed by air masses before reaching Bouvet Island. A detailed description of the parameters used to calculate the backward trajectories can be found in Text S1 of Supporting Information S1.

3. Results

3.1. The BOU Diatom Record

3.1.1. Diatom Abundance

A total of 10,852 diatom fragments and valves were found in the BOU between austral winters 2000–2015 CE, most of them being whole diatom valves (79%). Diatoms were mostly well preserved with many intact cells (i.e. 2 valves) and colonies of two to three cells (i.e. 4 to 6 valves).

The mean annual diatom abundance was 723.5 (n), with values ranging from 95 (n) (2004–2005 CE) to 3,127 (n) (2014–2015 CE) (Figure 2m). Negligible or weak but not statistically significant correlations were observed between the diatom abundance and both the volume of meltwater filtered per sample ($R = 0.36$, $p > 0.1$, $n = 14$) and the annual snow accumulation estimated from the BOU ($R = 0.08$, $p > 0.1$, $n = 14$). The mean annual diatom concentration was 2143.3 n L^{-1}, with values ranging from 553.9 n L^{-1} (2004–2005 CE) to 10,760.5 n L^{-1} (2014–2015 CE) (Figure S3 in Supporting Information S1). Both abundance and concentration presented a pronounced increase after 2012 CE and peaked in 2015 CE.

The annual total diatom abundance presented a strong and statistically significant correlation with the local mean wind speed in the Bouvet Island region ($R = 0.56$, $p < 0.05$, $n = 14$) (Figure 2n), and a high correspondence with wind speed anomalies (e.g., 2015 CE; Figure S4 in Supporting Information S1). Diatom abundance was negatively correlated with maximum chlorophyll concentrations ($R = -0.52$, $p < 0.1$, $n = 12$) over an extended region around Bouvet (including South Georgia). Non-statistically significant ($p > 0.1$), correlations were observed between the total diatom abundance and the local northernmost sea ice edge position ($R = 0.24$, $n = 14$), the mean ($R = -0.18$, $n = 12$) and maximum ($R = -0.13$, $n = 12$) chlorophyll concentrations close to Bouvet, and the mean chlorophyll concentration in the extended region ($R = -0.37$, $n = 12$).

The sub-annual total diatom concentration data from the BOU exhibited considerable variability both within and between the targeted years (Figure S5 in Supporting Information S1). Sub-annual total diatom concentrations reach a maximum increase of 108% (austral summer (JFM) 2003/2004) and a minimum decrease of 65% (JFM 2011/2012), in relation to the mean JFM diatom concentration (1,116 ± 662 n L^{-1}).

Among the total diatom fragments and valves counted in the BOU (2000–2015 CE), 8547 (Figure S6 in Supporting Information S1) were classified to the genus level or higher. A total of 40 diatom species and genus–taxon groupings were identified. Of them, 11 occurred at ≥2% relative abundance (Figure 2a and Figure S6 in Supporting Information S1). The main diatom assemblage is dominated by *Shionodiscus gracilis* (30.4%), *Fragilariopsis cylindrus* (16.2%), *Pseudo-nitzschia* spp. (9.6%), *F. pseudonana* (9.6%) (Figures 2b–2l and Figure S6 in Supporting Information S1). All species are extant in the modern SO.

The most abundant diatom in the BOU diatom assemblage was *S. gracilis*, an open ocean diatom species common in the SO (Crosta et al., 2005). Of the 11 taxa identified in the main diatom assemblage, seven are exclusively marine, while the other four have been identified in marine, freshwater, and brackish environments. The marine taxa identified contribute 86.4% to the main diatom assemblage and include open ocean species/groups (*S. gracilis*, *F. pseudonana*, *F. separanda*, *Pseudonitzschia* spp., and *Thalassiothrix* group) (Allen et al., 2020; Crosta et al., 2005; Rigual-Hernández et al., 2015; Zielinski & Gersonde, 1997), and sea-ice-affiliated diatoms (*F. cylindrus* and *F. curta*) (Lizotte, 2001; Zielinski & Gersonde, 1997). The four taxa associated with marine, freshwater, and brackish environments (*Luticola* cf. *muticopsis*, *Luticola* cf. *austroatlantica*, *Pinnularia* cf. *borealis* and *Cyclotella* group; Unconstrained taxa group-UTG) represent the remaining 13.6% of the main diatom assemblage.

The annual SIDI and n-SIDI concentration records present statistically significant ($p < 0.05$) correlations with the annual total diatom concentration ($R = 0.56$ and $R = 0.99$, respectively; Figure S3 in Supporting Information S1). The n-SIDI concentration presents similar values to the total diatom concentration, while the SIDI concentration is considerably lower.

Sub-annual diatom concentration subsets reveal two scenarios (Figure S5 in Supporting Information S1). The SIDI concentration parameter shows a strong seasonality with higher values during OND (1,112.6 ± 1,732.9 n L^{-1}) and lower ones during JFM (320.6 ± 514.8 n L^{-1}). Conversely, no consistent seasonality or trend is observed in the n-SIDI concentration record.

3.1.2. Environmental Correlations

The annual diatom abundance records (total, SIDI, and n-SIDI) are compared to environmental parameters over the 2000 to 2014 CE period (Figure 3). The total, SIDI and n-SIDI abundance records are all significantly ($p < 0.1$) correlated with annual wind speed over a region upwind from BOU, with maximum values of $R = 0.81$, $R = 0.86$ and $R = 0.77$, respectively. These positive correlations ($R \geq 0.46$) align over a latitudinal band (40°–50°S) extending between 10° and 45°W. The SIDI abundance record is also negatively correlated with annual wind speed over the northern Weddell Sea (Figure 3b). The total, SIDI and n-SIDI abundance records are

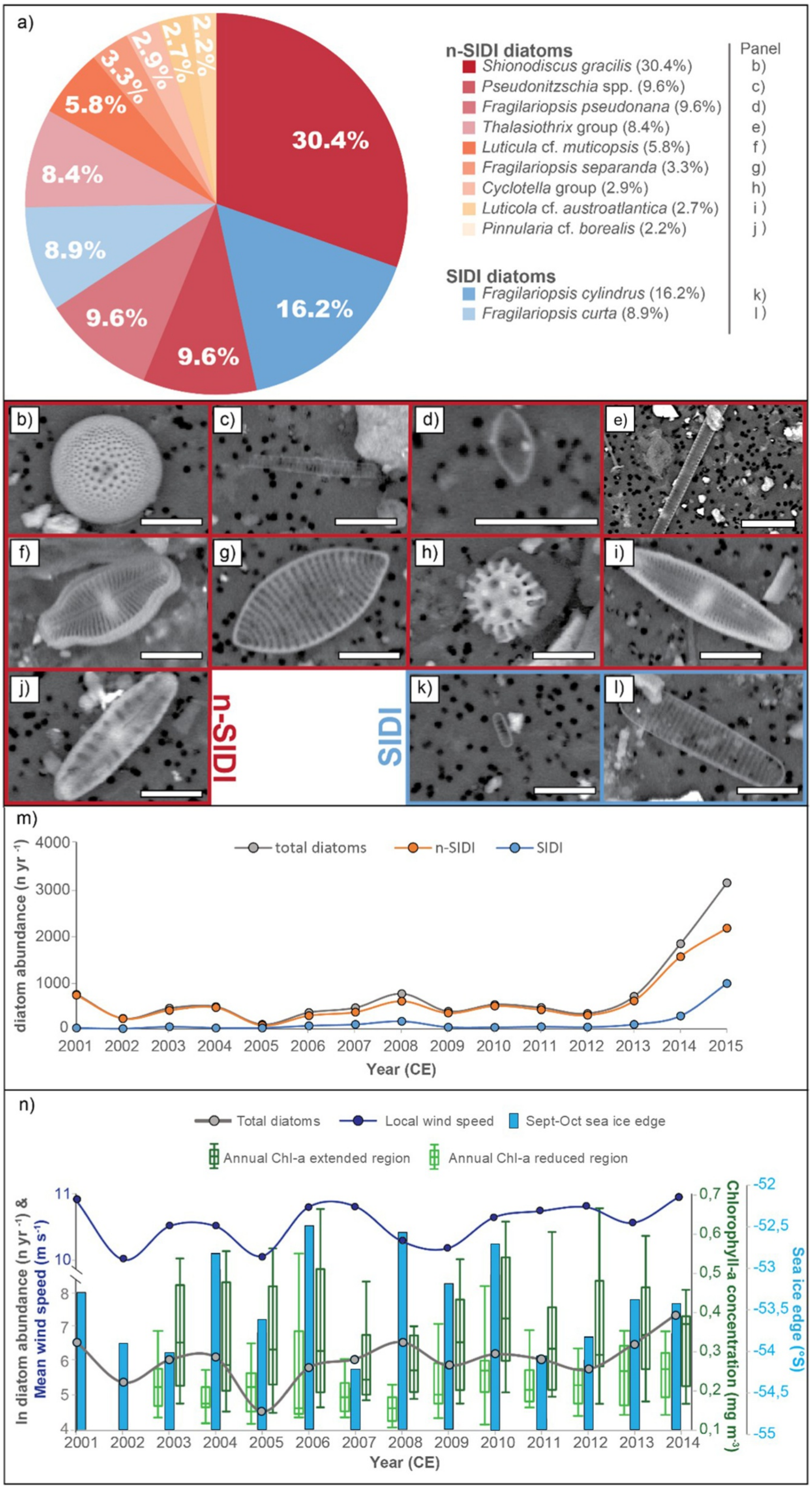

Figure 2. Diatom record from the BOU. (a) Main diatom assemblage composition of the BOU (2000–2015 CE). Percentages reported in this figure were normalized to the main species identified. (b–l) SEM micrographs of n-SIDI (b–j) and SIDI (k–l) diatoms from BOU main diatom assemblage. Scale bar in bottom right of each ((b–l) micrograph represents 10 μm. m) BOU diatom abundance time series for total diatoms and diatom subsets. (n) BOU total diatom abundance, local annual mean wind speed, September–October sea ice edge position and annual chlorophyll concentration time series.

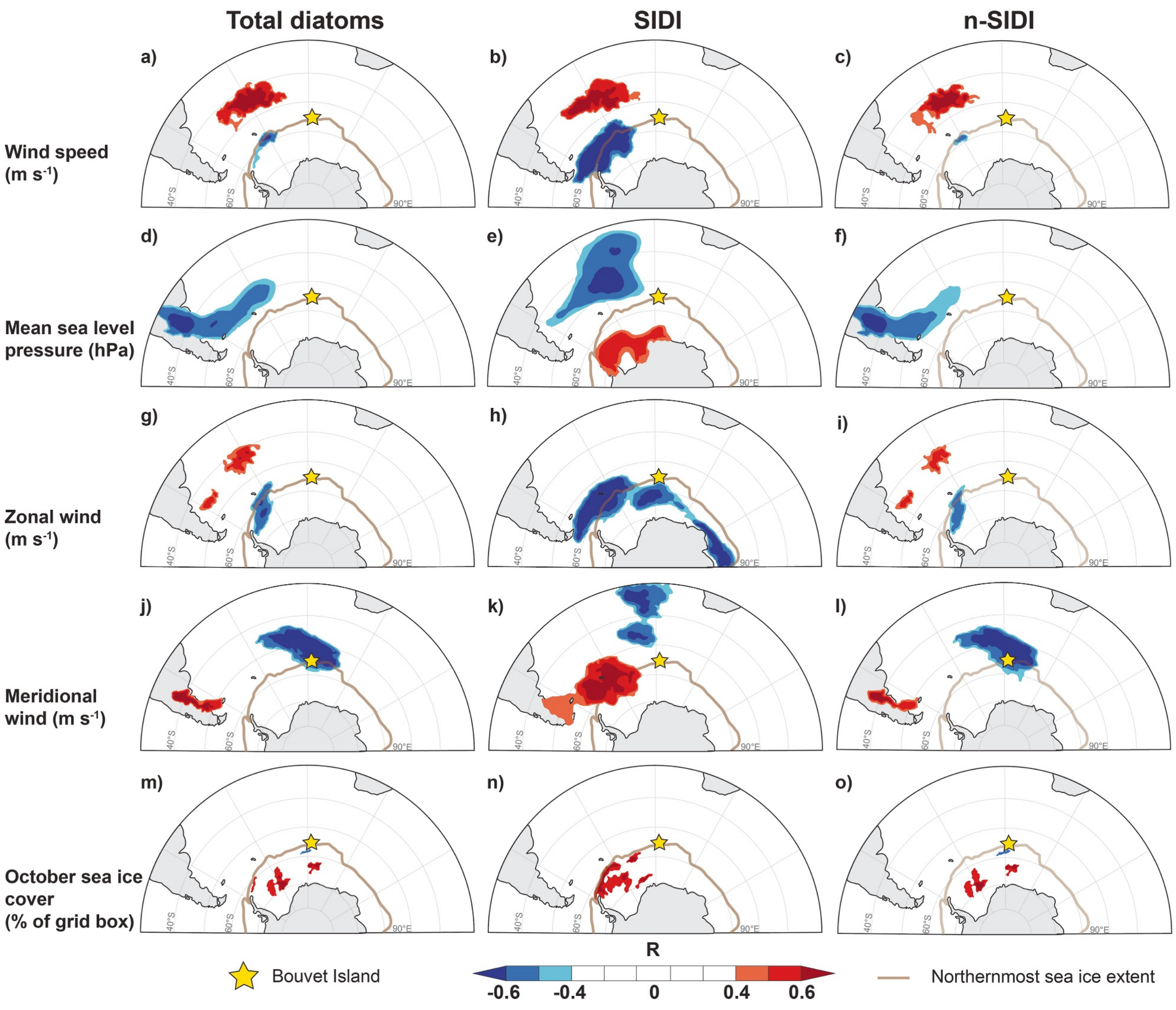

Figure 3. Regional maps showing spatial correlations between environmental parameters and annual diatom records over the 2000–2014 CE period (a–o). The colored areas indicate highly correlated regions ($R \geq 0.46$ or $R \leq -0.46$) ($p < 0.1$). The regional maps only present areas of spatial correlation larger than 1° × 1°.

significantly ($p < 0.1$) correlated with annual zonal wind speed over a region upwind from BOU. Among these correlations, the total and n-SIDI abundance records exhibit a transition at 50°S, with positive values to the north and negative values to the south. The total, SIDI and n-SIDI abundance records are significantly correlated ($p < 0.1$) with annual meridional wind speed over BOU, with negative correlations reaching $R = -0.86$, $R = -0.66$ and $R = -0.87$, respectively. Additionally, the SIDI abundance record presents a positive correlation with annual meridional wind speed over the northern Weddell Sea (Figure 3k). All annual diatom abundance records are significantly ($p < 0.1$) correlated with the annual mean sea level pressure over a wide region centered over the South Atlantic Ocean (40°–55°S, 20–60°W), with negative correlations reaching $R = -0.78$, $R = -0.65$ and $R = -0.79$ for total, SIDI and n-SIDI abundance records, respectively. The SIDI abundance record is significantly correlated ($p < 0.1$) with mean October sea ice cover in the north of the Weddell Sea ($R = 0.80$). No statistically significant ($p < 0.1$) large areas of strong correlations are identified between the total or n-SIDI annual diatom abundance records and the mean October sea ice cover surrounding BOU.

3.2. Air-Mass Back Trajectory Modeling

Backward trajectory analyses show that most of the air masses reaching Bouvet Island originate within the Atlantic sector of the SO. Annual and seasonal trajectories (Figure 1b and Figure S7 in Supporting

Information S1) exhibit similar patterns in which air masses (>2% frequency; Figure 1b) converge in a latitudinal band (50–60°S) stretching across the Antarctic Polar Front to the seasonal sea ice area. After converging in this region, air masses are channeled directly toward Bouvet Island.

4. Discussion

4.1. Diatom Source Region

The diatom record preserved in the BOU is mainly comprised (86.4%) of marine taxa from the pelagic SO (Crosta et al., 2005; Lizotte, 2001; Zielinski & Gersonde, 1997). This evidence suggests that the SO is the primary source of diatoms, as previously found in Antarctic ice cores, where diatom presence is attributed to entrainment and transport by winds (Allen et al., 2020; Budgeon et al., 2012; Tetzner, Allen, & Thomas, 2022). Backward trajectories confirm the majority of air masses reaching Bouvet Island travel over the western Atlantic Sector of the SO, upwind from Bouvet Island, therefore, establishing an efficient transport pathway for marine diatoms from the ocean surface to the BOU site (Figure 1b). The presence of diatom cells and preservation of delicate ornamentation suggest a rapid transport of diatoms from the surface ocean to Bouvet Island. Whilst the western region of the Atlantic sector of the SO is the likely source of diatoms to Bouvet Island, we cannot rule out minor contributions from other SO sectors.

Backward trajectories extend to potential sources for the UTG diatoms (13.6%), including Bouvet Island's coastline and landmasses upwind from Bouvet Island (e.g., South Georgia Island, South Sandwich Islands, Falkland Islands, and Patagonia) (Figure 1) (Kociolek et al., 2017; Lowe, 1975; Pinseel et al., 2020).

4.2. Enhanced Diatom Concentration

The BOU main diatom assemblage is consistent with assemblages reported from Antarctic Peninsula ice cores (Tetzner, Allen, & Thomas, 2022). However, BOU diatom concentrations are at least an order of magnitude higher than diatom concentrations reported from Antarctic sites (Tetzner, Thomas, et al., 2022).

The higher diatom concentrations in BOU compared with Antarctic ice cores, are likely due to the position within the SHWW belt, coupled with the expanse and proximity of open ocean. Strong winds enhance the production and transport of sea spray aerosols, including diatoms (Marks et al., 2019). Likewise, the proximity of Bouvet Island to its primary diatom source ensures direct short-range transport and deposition of marine aerosols. Conversely, marine diatoms preserved in Antarctic ice cores are transported greater distances and uplifted from sea level to elevations <1,000 m a.s.l. (Tetzner, Allen, & Thomas, 2022).

While strong winds produce the active entrainment and transport of diatoms, regional high primary productivity and the sea ice edge position enhance diatom availability at the sea surface. The South Atlantic sector of the SO is characterized by high primary productivity relative to the SO as a whole (Arrigo et al., 2008; Soppa et al., 2016). Although the vicinities of Bouvet are not particularly productive, the oceanic region upwind, where airmass trajectories reaching BOU converge, is one of the most productive open ocean regions in the SO (Soppa et al., 2016). High primary productivity likely increases the density of diatoms per unit area in the upper meters of the ocean, thereby increasing availability of diatoms for entrainment into aerosols and advection toward Bouvet. Conversely, diatoms found in ice cores from the West Antarctic Peninsula are primarily sourced from the Pacific sector of the SO (Allen et al., 2020; Tetzner, Allen, & Thomas, 2022), a region with comparatively lower diatom productivity (Soppa et al., 2016).

The sea ice edge position can also play a role in determining diatom availability in coastal low-elevation ice core sites where the primary diatom source is within the seasonal sea ice zone (Tetzner, Thomas, et al., 2022). The primary diatom source region to BOU is mostly the open ocean north of the seasonal sea ice edge, with an area of short-lived sea ice cover upwind of the island (Figure 1). This configuration means most of the source area is available for sea spray production year-round and likely enhances annual diatom concentrations. In contrast, the primary source of diatoms for coastal low-elevation sites along the West Antarctic Peninsula is the southern area of the seasonal sea ice zone, where the long-lasting (>8-month) sea ice cover limits the production of sea spray (Tetzner, Thomas, et al., 2022).

Overall, year-round entrainment and transport of diatoms by westerly winds are likely the main processes driving greater diatom concentrations in BOU, with high regional primary productivity and extended open ocean conditions at the diatom source region, upwind from Bouvet, enhancing diatom availability.

4.3. Drivers of BOU Annual Diatom Abundance Variability

The annual diatom abundance records reveal clear interannual variability and high correspondence with local wind strength variability and major anomalies (Figures 2m and 2n; Figure S4 in Supporting Information S1). Spatial correlations between annual diatom abundance records and atmospheric parameters (wind speed, wind vectors and mean sea level pressure) reveal a strong link between the presence of diatoms in BOU and regional atmospheric circulation (Figure 3). Strong winds enhance the production of marine aerosols (Marks et al., 2019), making marine diatoms available for regional atmospheric circulation transport. Our results are in close agreement with previous results from Antarctic ice core sites, where changes in the SHWW strength have been proposed as the main driver of diatom abundance variability (Allen et al., 2020; Budgeon et al., 2012; Tetzner, Allen, et al., 2025).

As previously mentioned, besides SHWW strength, SO primary productivity and sea ice dynamics could drive variability in BOU annual diatom abundance. Our results show there is no direct relationship between the annual diatom abundance and primary productivity in the vicinity of BOU. Furthermore, the negative correlation obtained between diatom abundance and primary productivity ($R = -0.48$; $p = 0.1$) over the extended region upwind from BOU is consistent with the negative influence of winds on primary productivity. Large phytoplankton blooms generally occur in well-stratified, stable surface waters (Lester et al., 2021; Swart et al., 2015). Strong winds break down surface stratification and allow cells to sink (Fitch & Moore, 2007). While strong SHWW partly inhibit bloom development, they enhance marine aerosol production. The limited influence of SO primary productivity driving the BOU diatom record's variability is further supported by the lack of the characteristic SO primary productivity seasonal timing in the BOU diatom record.

Sea ice dynamics impact the extent and duration of seasonal diatom blooms and, therefore, the availability of diatoms in the seasonal sea ice zone (Arrigo et al., 2008; Buchovecky et al., 2023). The location of BOU's primary open ocean diatom source (>2% back trajectory frequency; Figure 1b) overlaps with the northern-most extent of the seasonal sea ice zone, ensuring a short-lived sea ice influence on the BOU diatom records. This limited influence is further supported by diffuse and non-significant ($p > 0.1$) spatial correlations between both total and n-SIDI diatom abundances and the northernmost sea ice edge position around Bouvet; and the lack of a characteristic sea ice seasonality in the total and n-SIDI diatom concentration records. Despite the negligible influence of sea ice on the total and n-SIDI diatom abundance records, the SIDI abundance record (~25% of BOU's diatom assemblage) presented a strong relationship ($R = 0.8$) with sea ice cover and a characteristic sea ice seasonality. The influence of sea ice over the SIDI abundance record can be explained by the strong relationship between this diatom subset and a low-pressure center in the South Atlantic (Figure 3e), which promotes stronger southerly winds over the sea ice area in the NW Weddell Sea (Figure 3k), weaker winds at 50–60°S (30–60°W) (Figure 3h) and strong northerly winds north of Bouvet Island (Figure 3k). The enhanced southerlies and weakened westerlies favor the advection of cold air and sea ice to the northern Weddell Sea ice margin, thereby expanding the SIDI diatom source while actively extracting sea ice diatoms from the sea ice margin. The close relationship between the SIDI abundance record and the sea ice cover in the NW Weddell Sea (Figure 3n) highlights the potential of this diatom subset to inform about sea ice variability. Altogether, our results support that interannual atmospheric changes in the Atlantic sector of the SHWW belt are the main drivers of BOU diatom abundance variability.

4.4. Potential to Extend the BOU Record

The BOU diatom record (2000–2015 CE) is the first ice core diatom record to provide evidence of wind variability driving the entrainment of diatoms directly from their marine source region, in the core of the SHWW. The strong link between annual BOU diatom abundance and wind speed in the SW Atlantic showcases the potential of BOU diatom abundance as a proxy for reconstructing past changes in the SHWW. Over longer timescales, the total diatom abundance together with the SIDI:n-SIDI abundance ratio can provide insights into SHWW strength and migration. Despite BOU's potential, the recovery of a long ice core is complicated by Bouvet Island's past volcanic activity and the likelihood that past eruptions have distorted the ice cap and perturbed its climatic record (Thomas et al., 2021). Our results suggest that other, non-volcanic, sub-Antarctic islands could preserve valuable, intact paleoclimatic records (e.g., South Georgia; Isla Grande de Tierra del Fuego (Tetzner, Thomas, et al., 2025)).

5. Conclusions

Windblown particles preserved in ice cores can provide valuable records of past changes in atmospheric circulation. Our study confirms the presence of windblown diatoms in firn layers from BOU (2000–2015 CE). The BOU diatom record is mainly comprised of Southern Ocean marine taxa in numbers greater than at any other previously published ice core sites. This record provides the first evidence of the number and diversity of diatoms actively entrained by winds in the core of the SHWWs.

Our analysis of this diatom record demonstrates that temporal variability in diatom abundance is primarily driven by changes in wind strength in the core of the SHWWs. These findings highlight the diatom abundance record preserved in Bouvet Island as a novel proxy of interannual wind strength variability in the Atlantic sector of the SHWWs. Further research should prioritize analyses of ice core diatom records from the sub-Antarctic region over longer timescales to deliver annual resolution records of the SHWW—a vital driver of Antarctic climate variability.

Conflict of Interest

The authors declare no conflicts of interest relevant to this study.

Availability Statement

The data sets original to this work can be found in Tetzner et al. (2026), published in the UK Polar Data Centre (https://doi.org/10.5285/a6a1aa67-c906-4887-8983-8ef07897a74e).

Acknowledgments

We would like to thank Iris Buisman and Giulio Lampronti from the Microscopy Lab, Earth Sciences Department, University of Cambridge, for their technical support in the use of the SEM. We would like to thank the École Polytechnique Fédérale de Lausanne, the Swiss Polar Institute, and Ferring Pharmaceuticals Inc. for providing the initial funds to collect the Bouvet Island ice core (Grant subICE). We want to thank Xavier Crosta and Maaike Zwier for their constructive comments that led to an improved manuscript.

References

Aaboe, S., Down, E. J., Sørensen, A., Lavergne, T., & Eastwood, S. (2023). Sea-ice edge climate data record 1978-present, v3.0. *Copernicus Climate Change Service (C3S) Climate Data Store (CDS)*. https://doi.org/10.24381/cds.29c46d83

Allen, C. S., Thomas, E. R., Blagbrough, H., Tetzner, D. R., Warren, R. A., Ludlow, E. C., & Bracegirdle, T. J. (2020). Preliminary evidence for the role played by South westerly wind strength on the marine diatom content of an Antarctic Peninsula ice core (1980–2010). *Geosciences*, *10*(3), 87. https://doi.org/10.3390/geosciences10030087

Armand, L. K., Crosta, X., Romero, O., & Pichon, J.-J. (2005). The biogeography of major diatom taxa in Southern Ocean sediments: 1. Sea ice related species. *Palaeogeography, Palaeoclimatology, Palaeoecology*, *223*(1–2), 93–126. https://doi.org/10.1016/j.palaeo.2005.02.015

Arrigo, K. R., van Dijken, G. L., & Bushinsky, S. (2008). Primary production in the Southern Ocean, 1997–2006. *Journal of Geophysical Research*, *113*(C8). https://doi.org/10.1029/2007jc004551

Buchovecky, B., MacGilchrist, G. A., Bushuk, M., Haumann, F. A., Frölicher, T. L., Le Grix, N., & Dunne, J. (2023). Potential predictability of the spring bloom in the Southern Ocean sea ice zone. *Geophysical Research Letters*, *50*(20), e2023GL105139. https://doi.org/10.1029/2023gl105139

Budgeon, A. L., Roberts, D., Gasparon, M., & Adams, N. (2012). Direct evidence of Aeolian deposition of marine diatoms to an ice sheet, Antarct. *Science*, *24*(5), 527–535. https://doi.org/10.1017/S0954102012000235

Cefarelli, A. O., Ferrario, M. E., Almandoz, G. O., Atencio, A. G., Akselman, R., & Vernet, M. (2010). Diversity of the diatom genus fragilariopsis in the Argentine Sea and Antarctic waters: Morphology, distribution and abundance. *Polar Biology*, *33*(11), 1463–1484. https://doi.org/10.1007/s00300-010-0794-z

Crosta, X., Romero, O., Armand, L. K., & Pichon, J. J. (2005). The biogeography of major diatom taxa in Southern Ocean sediments: 2. Open ocean related species. *Palaeogeography, Palaeoclimatology, Palaeoecology*, *223*(1–2), 66–92. https://doi.org/10.1016/j.palaeo.2005.03.028

Deng, K., Azorin-Molina, C., Yang, S., Hu, C., Zhang, G., Minola, L., & Chen, D. (2022). Changes of Southern Hemisphere westerlies in the future warming climate. *Atmospheric Research*, *270*, 106040. https://doi.org/10.1016/j.atmosres.2022.106040

Fitch, D. T., & Moore, J. K. (2007). Wind speed influence on phytoplankton bloom dynamics in the southern ocean marginal ice zone. *Journal of Geophysical Research*, *112*(C8). https://doi.org/10.1029/2006jc004061

Flores-Aqueveque, V., Villaseñor, T., Gómez-Fontealba, C., Alloway, B. V., Alfaro, S., Pizarro, H., et al. (2024). Multisequal Aeolian deposition during the Holocene in southwestern Patagonia (51° S) was modulated by southern westerly wind intensity and vegetation type. *Quaternary Science Reviews*, *331*, 108616. https://doi.org/10.1016/j.quascirev.2024.108616

Gruber, N., Clement, D., Carter, B. R., Feely, R. A., Van Heuven, S., Hoppema, M., et al. (2019). The oceanic sink for anthropogenic CO_2 from 1994 to 2007. *Science*, *363*(6432), 1193–1199. https://doi.org/10.1126/science.aau5153

Harper, M. A., & McKay, R. M. (2010). Diatoms as markers of atmospheric transport. In E. F. Stoermer & J. P. Smol (Eds.), *The diatoms: Applications for the environmental and earth sciences* (pp. 552–559). Cambridge University Press. https://doi.org/10.1017/CBO9780511763175.032

Hasle, G. R., Syvertsen, E. E., & von Quillfeldt, C. H. (1996). Fossula Arcticagen. nov., spec. nov., a marine Arctic araphid diatom. *Diatom Research*, *11*(2), 261–272. https://doi.org/10.1080/0269249x.1996.9705383

Hersbach, H., & Dee, D. J. E. N. (2016). ERA5 reanalysis is in production. *ECMWF newsletter*, *147*, 5–6.

Jones, J. M., Gille, S. T., Goosse, H., Abram, N. J., Canziani, P. O., Charman, D. J., et al. (2016). Assessing recent trends in high-latitude Southern Hemisphere surface climate. *Nature Climate Change*, *6*(10), 917–926. https://doi.org/10.1038/nclimate3103

Keppler, L., & Landschützer, P. (2019). Regional wind variability modulates the Southern Ocean carbon sink. *Scientific Reports*, *9*(1), 7384. https://doi.org/10.1038/s41598-019-43826-y

King, A. C. F., Thomas, E. R., Pedro, J. B., Markle, B., Potocki, M., Jackson, S. L., et al. (2019). Organic compounds in a sub-Antarctic ice core: A potential suite of sea ice markers. *Geophysical Research Letters*, *46*(16), 9930–9939. https://doi.org/10.1029/2019gl084249

Kociolek, J. P., Kopalová, K., Hamsher, S. E., Kohler, T. J., Van de Vijver, B., Convey, P., & McKnight, D. M. (2017). Freshwater diatom biogeography and the genus Luticola: An extreme case of endemism in Antarctica. *Polar Biology*, *40*(6), 1185–1196. https://doi.org/10.1007/s00300-017-2090-7

Koffman, B. G., Goldstein, S. L., Winckler, G., Kaplan, M. R., Bolge, L., & Biscaye, P. (2023). Abrupt changes in atmospheric circulation during the medieval climate anomaly and little ice age recorded by Sr-Nd isotopes in the Siple dome ice core, Antarctica. *Paleoceanography and Paleoclimatology*, *38*(4), e2022PA004543. https://doi.org/10.1029/2022pa004543

Le Quéré, C., Rodenbeck, C., Buitenhuis, E. T., Conway, T. J., Langenfelds, R., Gomez, A., et al. (2007). Saturation of the Southern Ocean CO_2 sink due to recent climate change. *Science*, *316*(5832), 1735–1738. https://doi.org/10.1126/science.1136188

Lester, C. W., Wagner, T. J. W., McNamara, D. E., & Cape, M. R. (2021). The influence of meltwater on phytoplankton blooms near the sea-ice edge. *Geophysical Research Letters*, *48*(2), e2020GL091758. https://doi.org/10.1029/2020gl091758

Lizotte, M. P. (2001). The contributions of sea ice algae to Antarctic marine primary production. *American Zoologist*, *41*(1), 57–73. https://doi.org/10.1093/icb/41.1.57

Lowe, R. L. (1975). Comparative ultra structure of the valves of some Cyclotella species (bacillariophyceae). *Journal of Phycology*, *11*(4), 415–424. https://doi.org/10.1111/j.1529-8817.1975.tb02805.x

Marks, R., Górecka, E., McCartney, K., & Borkowski, W. (2019). Rising bubbles as mechanism for scavenging and aerosolization of diatoms. *Journal of Aerosol Science*, *128*, 79–88. https://doi.org/10.1016/j.jaerosci.2018.12.003

Medley, B., & Thomas, E. R. (2019). Increased snowfall over the Antarctic ice sheet mitigated twentieth-century sea-level rise. *Nature Climate Change*, *9*(1), 34–39. https://doi.org/10.1038/s41558-018-0356-x

Moore, J. K., & Abbott, M. R. (2000). Phytoplankton chlorophyll distributions and primary production in the Southern Ocean. *Journal of Geophysical Research*, *105*(C12), 28709–28722. https://doi.org/10.1029/1999jc000043

Perren, B. B., Hodgson, D. A., Roberts, S. J., Sime, L., Van Nieuwenhuyze, W., Verleyen, E., & Vyverman, W. (2020). Southward migration of the Southern Hemisphere westerly winds corresponds with warming climate over centennial timescales. *Communications Earth & Environment*, *1*(1), 58. https://doi.org/10.1038/s43247-020-00059-6

Pinseel, E., Janssens, S. B., Verleyen, E., Vanormelingen, P., Kohler, T. J., Biersma, E. M., et al. (2020). Global radiation in a rare biosphere soil diatom. *Nature Communications*, *11*(1), 2382. https://doi.org/10.1038/s41467-020-16181-0

Pritchard, H. D., Arthern, R. J., Vaughan, D. G., & Edwards, L. A. (2009). Extensive dynamic thinning on the margins of the Greenland and Antarctic ice sheets. *Nature*, *461*(7266), 971–975. https://doi.org/10.1038/nature08471

Riaux-Gobin, C., Poulin, M., Dieckmann, G., Labrune, C., & Vétion, G. (2011). Spring phytoplankton onset after the ice break-up and sea-ice signature (Adélie Land, East Antarctica). *Polar Research*, *30*(1), 5910. https://doi.org/10.3402/polar.v30i0.5910

Rigual-Hernández, A. S., Trull, T. W., Bray, S. G., Cortina, A., & Armand, L. K. (2015). Latitudinal and temporal distributions of diatom populations in the pelagic waters of the subantarctic and polar frontal zones of the Southern Ocean and their role in the biological pump. *Biogeosciences*, *12*(18), 5309–5337. https://doi.org/10.5194/bg-12-5309-2015

Saunders, K. M., Roberts, S. J., Perren, B., Butz, C., Sime, L., Davies, S., et al. (2018). Holocene dynamics of the Southern Hemisphere westerly winds and possible links to CO_2 outgassing. *Nature Geoscience*, *11*(9), 650–655. https://doi.org/10.1038/s41561-018-0186-5

Soppa, M. A., Völker, C., & Bracher, A. (2016). Diatom phenology in the southern ocean: Mean patterns, trends and the role of climate oscillations. *Remote Sensing*, *8*(5), 420. https://doi.org/10.3390/rs8050420

Swart, S., Thomalla, S. J., & Monteiro, P. M. (2015). The seasonal cycle of mixed layer dynamics and phytoplankton biomass in the Sub-Antarctic Zone: A high-resolution glider experiment. *Journal of Marine Systems*, *147*, 103–115. https://doi.org/10.1016/j.jmarsys.2014.06.002

Tamhane, J., Thomas, Z. A., Cadd, H., Harris, M. R., Turney, C., Marjo, C. E., et al. (2023). Mid-Holocene intensification of Southern Hemisphere westerly winds and implications for regional climate dynamics. *Quaternary Science Reviews*, *305*, 108007. https://doi.org/10.1016/j.quascirev.2023.108007

Tetzner, D., Allen, C., & Thomas, E. (2026). Annual diatom abundance and seasonal diatom concentration from the Bouvet Island firn core, Antarctic Peninsula, 2000–2015 (version 1.0) [Dataset]. *NERC EDS UK Polar Data Centre*. https://doi.org/10.5285/a6a1aa67-c906-4887-8983-8ef07897a74e

Tetzner, D., Thomas, E., & Allen, C. (2019). A validation of ERA5 reanalysis data in the Southern Antarctic Peninsula—Ellsworth land region, and its implications for ice core studies. *Geosciences*, *9*(7), 289. https://doi.org/10.3390/geosciences9070289

Tetzner, D., Thomas, E. R., Allen, C. S., & Wolff, E. W. (2021). A refined method to analyze insoluble particulate matter in ice cores, and its application to diatom sampling in the Antarctic Peninsula. *Frontiers in Earth Science*, *9*, 617043. https://doi.org/10.3389/feart.2021.617043

Tetzner, D. R., Allen, C. S., & Thomas, E. R. (2022). Regional variability of diatoms in ice cores from the Antarctic Peninsula and Ellsworth Land, Antarctica. *The Cryosphere*, *16*(3), 779–798. https://doi.org/10.5194/tc-16-779-2022

Tetzner, D. R., Allen, C. S., Thomas, E. R., Wolff, E. W., & Franzke, C. L. (2025). Timing of the recent migration and intensification of the Southern Hemisphere westerly winds. *Geophysical Research Letters*, *52*(13), e2024GL113672. https://doi.org/10.1029/2024gl113672

Tetzner, D. R., Thomas, E. R., Allen, C. S., & Grieman, M. M. (2022). Regional validation of the use of diatoms in ice cores from the Antarctic Peninsula as a Southern Hemisphere westerly wind proxy. *Climate of the Past*, *18*(7), 1709–1727. https://doi.org/10.5194/cp-18-1709-2022

Tetzner, D. R., Thomas, E. R., Allen, C. S., McCulloch, R. D., Perren, B. B., McGuire, A., et al. (2025). The first firn core from the Cordillera Darwin Icefield: Implications for future ice core research. *Journal of Geophysical Research: Atmospheres*, *130*(12), e2024JD043124. https://doi.org/10.1029/2024jd043124

Thomas, E. R., Gacitúa, G., Pedro, J. B., Faith King, A. C., Markle, B., Potocki, M., & Moser, D. E. (2021). Physical properties of shallow ice cores from Antarctic and sub-Antarctic islands. *The Cryosphere*, *15*(2), 1173–1186. https://doi.org/10.5194/tc-15-1173-2021

Thomas, E. R., Tetzner, D., Markle, B., Pedro, J., Gacitúa, G., Moser, D. E., & Jackson, S. (2024). The first firn core from Peter I Island–capturing climate variability across the Bellingshausen Sea. *Climate of the Past*, *20*(11), 2525–2538. https://doi.org/10.5194/cp-20-2525-2024

Warnock, J. P., & Scherer, R. P. (2015). Diatom species abundance and morphologically-based dissolution proxies in coastal Southern Ocean assemblages. *Continental Shelf Research*, *102*, 1–8. https://doi.org/10.1016/j.csr.2015.04.012

Zielinski, U., & Gersonde, R. (1997). Diatom distribution in Southern Ocean surface sediments (Atlantic sector): Implications for paleoenvironmental reconstructions. *Palaeogeography, Palaeoclimatology, Palaeoecology*, *129*(3–4), 213–250. https://doi.org/10.1016/s0031-0182(96)00130-7

10.1029/2026GL121625

References From the Supporting Information

Draxler, R. R., & Hess, G. D. (1998). An overview of the HYSPLIT_4 modelling system for trajectories. *Australian Meteorological Magazine*, *47*(4), 295–308. https://doi.org/10.1071/es98032

Stein, A. F., Draxler, R. R., Rolph, G. D., Stunder, B. J., Cohen, M. D., & Ngan, F. (2015). NOAA's HYSPLIT atmospheric transport and dispersion modeling system. *Bulletin of the American Meteorological Society*, *96*(12), 2059–2077. https://doi.org/10.1175/bams-d-14-00110.1